

SIMULATION OF THE SELECTIVE OXIDATION OF N-BUTANE TO MALEIC ANHYDRIDE IN A RISER/REGENERATOR SYSTEM

*Anja Püttmann, Ernst-U. Hartge, Joachim Werther
Hamburg University of Technology, Germany*

Abstract

A simulation tool is presented that is able to estimate the behavior of fluidized-bed reactors. A population balance approach is used to determine the particle size distribution within the reactor in stationary state. The model allows to describe the individual fate of particles in terms of attrition (abrasion and shrinkage) and transport effects. The fluidized-bed reactor modeling is based upon the Werther and Wein model for bubble growth [1] and simple kinetic approaches. The implementation within the framework of a flowsheet simulation software for solids processes allows for the flexible coupling of process models.

As an example the simulation of the selective oxidation of n-butane to maleic anhydride in a riser/regenerator system is presented and compared to measurements by Golbig and Werther on the laboratory scale [2]. The arrangement has been described by coupling a riser model with a bubbling fluidized-bed model. The simulation results turn out to be in good agreement with the measurements. Calculations show that high solids circulation rates are necessary. The importance of the catalyst's attrition-resistance and oxygen-load capacities for the economic success of the investigated technology is illustrated.

Introduction

For the design of processes involving fluids it is common today to use flowsheet simulation tools (e.g. [3]). There are several established program packages such as Aspen Plus. However, there are no flowsheet simulation tools on the market that can handle dependent and secondary dependent attributes of solids. SolidSim is a system for the steady-state simulation of solids processes that has been developed led by Hamburg University of Technology and a group of 11 institutes from 9 German universities [4]. It provides all the necessary structures required for the description of solids and the steady-state simulation of solids processes including physical treatment, thermal treatment, and also for reactions. The calculation follows the sequential-analytical mode: The individual unit models are calculated separately but with an automation of information transfer between them. Loops are solved iteratively. SolidSim contains already a lot of modules e.g. agglomeration, crystallization, comminution, classification, and solid-liquid separation but not yet reaction.

In the present work a fluidized bed reactor module is developed for the use in SolidSim. The fluidized bed reactor has a lot of advantages: excellent gas-solid contacting, no hot spots even with highly exothermal reactions, good gas-to-particle and bed-to-wall heat transfer and the ease of solids handling which is particularly important if the catalyst is quickly ageing. However, the list of disadvantages is as long: broad residence time distribution of the gas due to dispersion and gas-bypass in the form of bubbles, broad residence time distribution of solids due to intense mixing, erosion of bed internals and the attrition of the catalyst particles.

A particular disadvantage of the fluidized bed reactor is its difficult scale-up. In modern process design modeling and simulation tools can support scale-up calculations. A

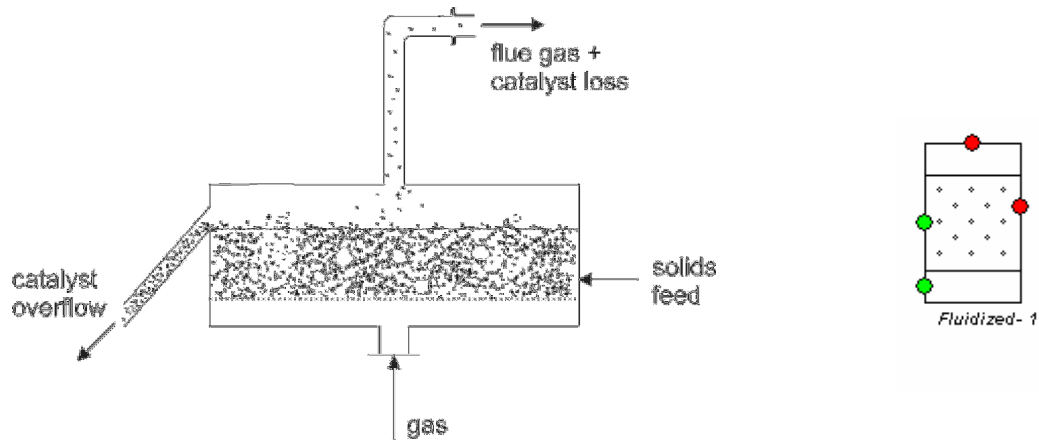


Fig. 1 Fluidized bed reactor module (left) SolidSim icon (right)

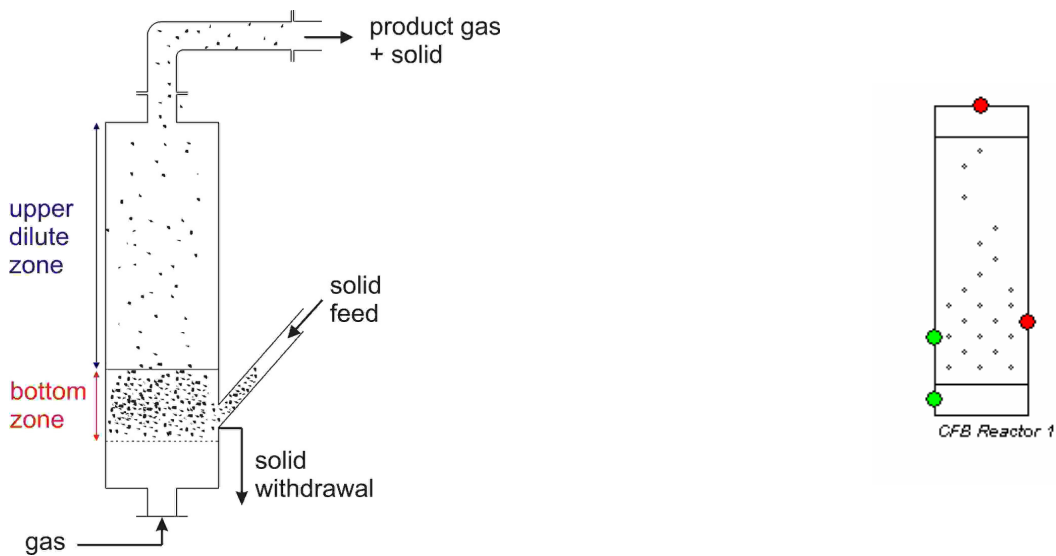


Fig. 2 Circulating fluidized bed reactor module (left) SolidSim icon (right)

modeling tool for the planning and designing of a technical fluidized bed reactor has to fulfill a lot of requirements. It should be able to describe the influence of the several changes which are typical for the scale-up process, for example enlargement of bed diameter, bed height and fluidizing velocity, and changes of gas distributor design.

The new fluidized-bed reactor integrated in the SolidSim package provides these functions. Its embedment into a general flowsheet simulation tool for solids processes allows for considering the effects of changes in the fluidized-bed reactor design and operating conditions, and the effects of changes in the configuration of other process units (e.g. gas cyclones) or in the configuration of the process structure as well. Likewise, the influence of changes in the fluidized-bed reactor configuration and operating conditions on any other process values can be estimated.

In this work the new SolidSim fluidized-bed reactor module will be applied to calculate the partial oxidation of n-butane to maleic anhydride (MA). The reaction takes place in a closed loop consisting of a circulating fluidized-bed riser, a bubbling fluidized-bed, and a gascyclone for solids recycle to the riser. The simulation results are validated by measurements by Golbig [2], [5]. The influence of an enlarged regenerator geometry on the reaction conversion and selectivity is demonstrated.

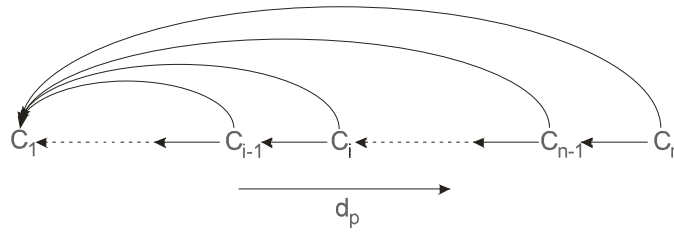


Fig. 3 Abrasion-induced mass transfer between particle size intervals.

Theory

SolidSim provides for the bubbling fluidized bed reactor and the circulating fluidized bed reactor one module each. The general layout of the modules is depicted in figs. (1) and (2).

Fluid dynamics of the bubbling fluidized-bed

Fluid dynamics are calculated according to the model of bubble growth by Hillgardt and Werther [6] and its later extension by Werther and Wein [1]. The latter work considers the combined action of coalescence and splitting of the bubbles. The initial bubble size is given by a correlation according to Davidson and Harrison [7]. The entrainment flux may be calculated from Geldart and Tasirin's work [8]. It is assumed that the level of the freeboard height exceeds the Transport Disengaging Height (TDH).

Fluid dynamics of the circulating fluidized-bed

The circulating fluidized bed reactor model divides the reactor into a bottom bed and the upper dilute zone (fig. 2). The bottom zone is modeled as a bubbling fluidized bed. Above the bottom bed the solids volume concentration for each particle size interval decays exponentially as proposed by Kunii and Levenspiel [9]. This leads to a classifying effect with respect to particle size.

Population balance for the fluidized-bed reactor

Focusing on a discretized particle size distribution the particular effect of abrasion may be illustrated with fig. 3. During the time interval Δt considered, a mass $m_{att,i}$ of fines is transferred from the size interval C_i into the smallest size interval C_1 , which collects all abrasion-produced fines. It can be assumed that all particles of the size interval C_i are involved in the generation of these fines. As a consequence, all particles are shrinking and some of them become smaller than the lower bound of their size interval. They must thus be assigned to the smaller size interval C_{i-1} . The mass transferred between neighboring intervals is denoted by $m_{i,i-1}$.

On the other hand, the rest of the material remains in its original size interval, even though the particles are also reduced in size. These phenomena of particle transfer can be summarized in a set of population balances the size fractions with index $2 \dots n$,

$$dm_i = -m_{att,i} - m_{i,i-1} + m_{i+1,i} \quad i = 2 \dots (n-1) \quad (1)$$

where n denotes the number of size intervals. The interval of the finest particles C_1 receives in addition to the shrunk mother particles from particle size interval C_2 all abrasion-produced fines from the other particle size intervals.

$$dm_1 = \sum_{i=2}^n m_{att,i} + m_{2,1} \quad (2)$$

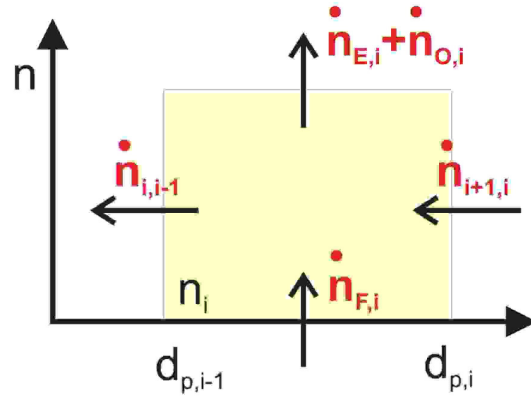


Fig. 4 Population balance for particle size interval i .

The particle size interval of the coarsest particles C_n receives no shrunk mother particles as there are no particles present in the system with a particle diameter that exceeds the particle diameter which defines the upper border of C_n .

$$dm_n = -m_{att,n} - m_{n,n-1} \quad (3)$$

In order to apply the defined set of mass balances (equs. (1) – (3)) the mass transfer to the neighboring size interval $m_{i,i-1}$ as well as the mass loss rate of fines $m_{att,i}$ must be available for each particle size interval i .

The mass rate of particles transferred to the neighboring size interval due to shrinkage of mother particles caused by abrasion can be obtained from population balances that apply in the steady-state (fig.4). Assuming that attrition follows the mode of pure abrasion, as described above, and no breakage takes place the number of mother particles in each particle size interval remains constant over time when the steady-state is reached. This applies to all particle size intervals $2 \dots n$ with the exception of particle size interval C_1 which collects the abrasion-produced fines from the particle size intervals C_2 through C_n . Thus, for the steady-state it can be formulated for particle size intervals 2 through $(n-1)$:

$$\frac{dn_i}{dt} = \dot{n}_{i+1,i} + \dot{n}_{F,i} - \dot{n}_{i,i-1} - \dot{n}_{O,i} - \dot{n}_{E,i} = 0 \quad i = 2 \dots (n-1) \quad (4)$$

and,

$$\frac{dn_i}{dt} = \dot{n}_{F,i} - \dot{n}_{i,i-1} - \dot{n}_{O,i} - \dot{n}_{E,i} = 0 \quad i = n \quad (5)$$

for particle size interval C_n respectively.

The population balance for particle size interval C_1 is not needed to determine the $n-1$ transfer fluxes of particles in between the n particle size intervals. The mass loss rate due to attrition, $\dot{m}_{att,p,i}$ for a single particle in the particle size interval i is related to the mass loss rate $\dot{m}_{att,i}$ of all particles in particle size interval i by:

$$\dot{m}_{att,p,i} = \frac{\dot{m}_{att,i}}{N_{p,i}} \quad (6)$$

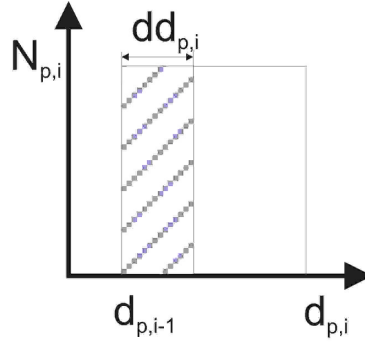


Fig. 5 Number of mother particles that leave particle size interval i per time interval dt due to shrinkage caused by evenly distributed attrition of fines from the particle surface.

If spherical particles with particle diameter d_p are assumed this number can be calculated from the total mass m_b of all particles in the system and the mass fraction $\Delta Q_{3,i}$:

$$N_{p,i} = \frac{6 \cdot m_b \cdot \Delta Q_{3,i}}{\pi \cdot d_{p,i}^3 \cdot \rho_s} \quad (7)$$

where ρ_s denotes the catalyst's apparent density.

It is assumed that abrasion follows the mode of fines being evenly removed from the surface of spherical mother particles so that after time interval dt the outer "shell" of the mother particle is abraded. It follows that the decrease rate of the mother particle diameter relates to the mass loss rate $\dot{m}_{att,p,i}$ of the single particle by:

$$\dot{m}_{att,p,i} = \frac{dd_{p,i}}{dt} \cdot \bar{d}_{p,i}^2 \cdot \pi \cdot \rho_s \quad (8)$$

From the graphical representation in fig.5 it can be seen that the number of particles $n_{i,i-1}$ that is transferred from particle size interval C_i to C_{i-1} by the end of a time interval Δt i.e. at the time $t+\Delta t$ can be obtained by:

$$n_{i,i-1} = \frac{d_{p,i,t} - d_{p,i,t+\Delta t}}{d_{p,i} - d_{p,i-1}} \cdot N_{p,i} \quad (9)$$

This expression is also valid when expressed in rates:

$$\dot{n}_{i,i-1} = \frac{dd_{p,i}}{dt} \cdot \frac{1}{d_{p,i} - d_{p,i-1}} \cdot N_{p,i} \quad (10)$$

Rearranging and inserting equ. 6 and 9 into equ. 10 yields:

$$\dot{n}_{i,i-1} = \frac{\dot{m}_{att,i}}{d_{p,i}^2 \cdot \pi \cdot \rho_s} \cdot \frac{1}{d_{p,i} - d_{p,i-1}}$$

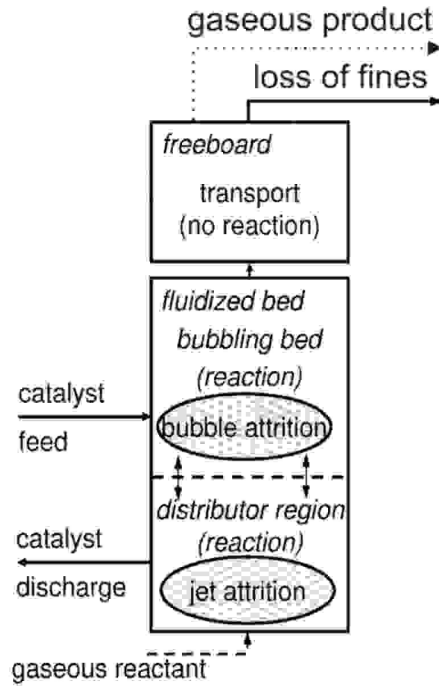


Fig. 6 Layout of a fluidized bed reactor model with attrition.

Attrition in the fluidized-bed reactor

Attrition in the fluidized-bed is assumed to be restricted to the jetting region and to the bulk of the bubbling bed (fig.6). Attrition in the freeboard is as a first approximation neglected. The jetting region is given by the penetration depth of the jets. From jet attrition in the n_{or} jets we obtain according to [10] a mass production of fines resulting from the size fraction i .

$$\dot{m}_{att,jett,i} = n_{or} \cdot c_j \cdot \bar{d}_{p,i} \cdot \rho_f \cdot \bar{d}_{or}^2 \cdot u_{or}^3 \cdot \Delta Q_{2,i} \quad (11)$$

Attrition due to bubbles is given by [11]

$$\dot{m}_{att,bubble,i} = c_b \cdot \bar{d}_{p,i} \cdot m_b \cdot (u - u_{mf})^3 \cdot \Delta Q_{2,i} \quad (12)$$

The mass loss rate of particle size interval i is simply the sum of the respective mass loss rates related to bubble and jet attrition.

$$\dot{m}_{att,i,Bett} = \dot{m}_{att,jett,i} + \dot{m}_{att,bubble,i} \quad (13)$$

Reaction

The model of the chemical conversion in the bubbling fluidized bed is based on the following simplifying assumptions:

- The fluidized bed is divided into two phases. One phase is the disperse solid-free phase which includes bubbles and grid jets. The other phase is the continuous suspension phase which surrounds the jets and bubbles.

- The bed inventory solids belong to the Geldart group A of powders. For such powders under technical operating conditions the superficial velocity u in the fluidized bed will always be much greater than the minimum fluidizing velocity u_{mf} . As a consequence the throughflow velocity in the suspension phase is with sufficient accuracy described by $(u_{mf}/\varepsilon_{mf})$ with ε_{mf} being the bed porosity under minimum fluidization conditions.
- Plug flow of gas is assumed in both phases.
- Mass transfer between the bubble and suspension phases is described by a correlation suggested by Sit and Grace [12]

$$k_G = \frac{u_{mf}}{3} + \sqrt{\frac{4D\varepsilon_{mf}u_b}{\pi d_v}} \quad (14)$$

where k_G is a height-dependent mass transfer coefficient which is based on unit reactor volume. d_v and u_b are the local mean bubble size and rise velocity, respectively.

- No change in volumetric gas flow due to reaction is considered (this effect has been taken into account e.g. by Sitzmann et al.[13])

Following these assumptions, the mass balances on a reactor volume element $dh \cdot A_R$ in the bubble phase yields for the steady-state:

$$\frac{\partial C_b}{\partial h} [u - u_{mf}(1 - \varepsilon_b)] + k_G a (C_b - C_d) = 0 \quad (15)$$

For the case of a first-order heterogeneously catalyzed reaction in the suspension phase we obtain in the dense phase:

$$\frac{dC_d}{dh} [u_{mf}(1 - \varepsilon_b)] - k_G a (C_b - C_d) - k_m (1 - \varepsilon_b) c_v \rho_p C_d = 0 \quad (16)$$

C_b and C_d are the reactant concentrations in the solid-free and suspension phases, respectively, k_m is the reaction rate constant of the first-order chemical reaction.

In the circulating fluidized bed reactor the bottom bed is modeled as a bubbling-fluidized bed as described above. In the upper dilute zone for the gas phase plug flow is assumed. The solids are perfectly mixed for each particle size interval above the total reactor height. The reactant concentration in the upper dilute zone is obtained from the respective reactant concentrations in the dense bottom zone at height H_b , the level above the distributor plate at which the exponential decay of the solids concentration starts:

$$C_{u,H_d} = \frac{C_{b,H_b} \cdot u_{b,H_b} \cdot \varepsilon_{b,H_b} + C_{d,H_b} \cdot u_{mf} \cdot (1 - \varepsilon_{b,H_b})}{u} \quad (17)$$

It follows for the mass balance on a reactor volume element $dh \cdot A_R$ in the upper dilute zone:

$$\frac{dC_d}{dh} = \frac{k_m \cdot (1 - \varepsilon_b) \cdot c_v \cdot \rho_p \cdot C_d}{u} \quad (18)$$

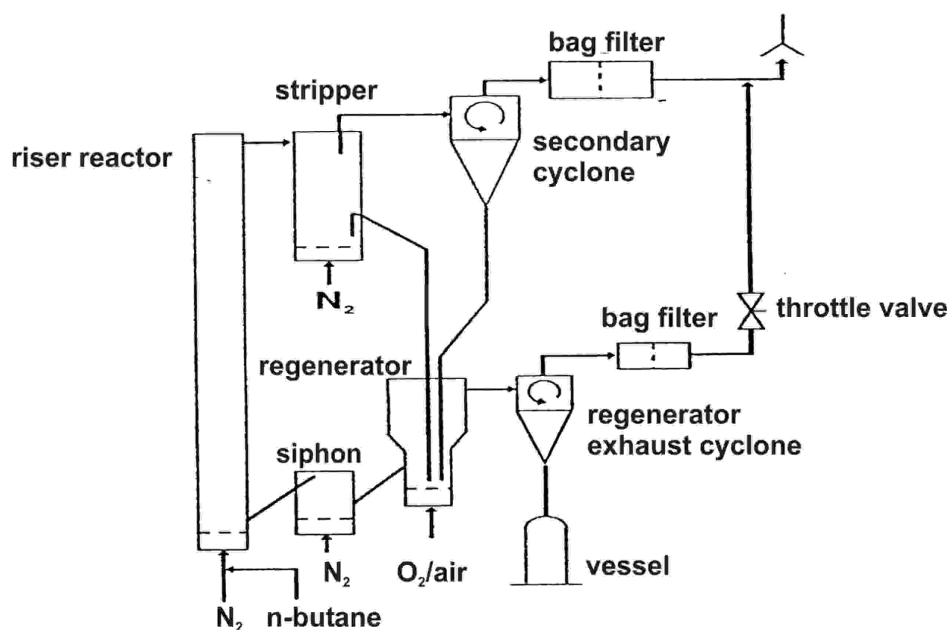


Fig. 7 Flowsheet of the laboratory circulating fluidized-bed facility used by Golbig [2].

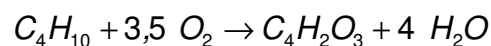
Although it may be significant in some cases chemical reaction in the freeboard region of the bubbling fluidized bed and inside the cyclone is neglected in the present work. The fluidized-bed reactors are supposed to be in steady-state and under isothermal operation.

Results and Discussion

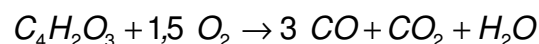
Definition of the test system

Maleic Anhydride (MA) is a raw product for many chemical products such as fibre-reinforced plastics in automotive and aviation industry, alkyd resin in paint and varnish, fumaric acid in food industry, pesticides and lube oil additives. The large variety of applications indicates that the synthesis of MA is of considerable economic interest.

The selective oxidation of MA in fixed bed or fluidized bed reactors is conventionally characterized by the presence of oxygen gas and hydrocarbon vapor at the active sites of the catalyst. Besides the partial oxidation of n-butane



in the presence of oxygen an undesired complete oxidation may occur,



In order to increase the selectivity it has been suggested (e.g. [14], [15]) to separate the reaction in two parts; i.e. a first step where the catalyst chemisorbs oxygen and a second step where the oxidized catalyst reacts with the hydrocarbons.

Golbig [5] and Golbig and Werther [2] published measurements that they obtained from operating a reactor/regenerator system for the oxidation of n-butane to MA on the laboratory scale. The experimental setup is depicted in fig.7. In the present work the

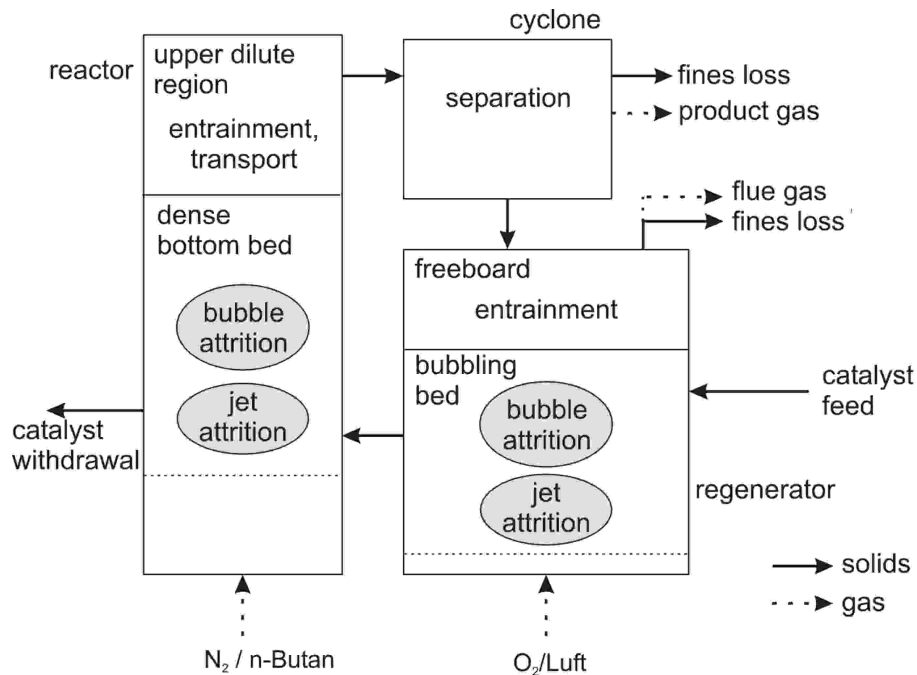


Fig. 8 Modeling steps in the solids loop.

Golbig/Werther configuration will be simulated using the flowsheet simulation tool SolidSim. The simulation results will be compared to the measurements.

The modeling of the riser/regenerator system is restricted to the main process units. The model layout is presented in fig.8. Configuration data for the modeled process units are taken from Golbig [5] and Golbig and Werther [2]: The riser reactor has a diameter of 21 mm and a 2820 mm. The regenerator diameter measures 51 mm and the regenerator height is 877mm. Whereas the freeboard section in the Golbig and Werther work has a diameter of 102mm in the simulation the regenerator diameter remains constant. The riser reactor is operated in the circulating fluidized bed mode with the superficial gas velocity $u_R=2\text{m/s}$ and the regenerator is operated in the bubbling bed mode with the superficial gas velocity $u_{Reg}=0.1\text{ m/s}$ respectively. The riser fluidization gas consists of nitrogen and n-butane. The regenerator fluidization gas is a mixture of oxygen and air. The solids inventory of the fluidized bed reactors can be obtained from measurements of the pressure drop. The simulated process operation conditions are 1bar and 450°C.

The gas cyclone has been designed using the SolidSim gas cyclone module which is based on the design rules in the VDI Heat Atlas [16]. As a result the main diameter of the gas cyclone is 20 mm, the vortex finder tube 10 mm, and the total height 30 mm. The gas cyclone has a pressure drop of 920 Pa.

For the standpipes plug flow of the solids is assumed and attrition in the standpipes is neglected. Therefore the steady state of the system does not depend on the design of the standpipes at all.

Tab. 1 gives an overview over the feed streams. As SolidSim is a steady state simulation tool and solids constantly leave the system (fig.8) a continuous catalyst feed is needed. Furthermore, the catalyst is assumed to have an initial oxygen load as it had extensive contact with aerial oxygen before it enters the system.

The catalyst is of the VPO-type with a Sauter diameter of about 31 μm and an apparent density of 1445 kg/m³ [2]. The parameters of the attrition characteristics are $C_j=9.5 \times 10^{-6}\text{ s}^2/\text{m}^3$ for jet-induced attrition and $C_b= 0.4 \times 10^{-3}\text{ s}^2/\text{m}^4$.

Tab.1 Feed data

	mass flow [g/s]	catalyst load [g O ₂ /g cat]
catalyst feed	8.0	0.8
regenerator gas feed	0.135	n/a
riser gas feed	0.373	n/a

Reaction rates are also obtained from Golbig [5]. For the oxidation of n-butane to MA in the riser reactor the effective reaction rate coefficient k_m in equs. (16) and (18) is substituted by:

$$k_{m,B} = k_{R,B} \cdot \bar{\xi}_R \quad (19)$$

where $\bar{\xi}_R$ is the average oxygen loading of the catalyst in the riser in g O₂/kg cat and $k_{R,B}$ is given by:

$$k_{R,B} = 62 \frac{m^3}{kg \cdot s} \cdot \exp\left(-\frac{6734K}{T}\right) \quad (20)$$

For the side-reaction, i.e. the complete oxidation of MA, k_m in equs. (16) and (18) is simply given by:

$$k_{m,MA} = 1,5 \frac{m^3}{kg \cdot s} \cdot \exp\left(-\frac{3735K}{T}\right) \quad (21)$$

For the re-oxidation of the catalyst in the regenerator has to be replaced by equ. (16):

$$\frac{dC_{O_2,d}}{dh} = \frac{k_G \cdot a \cdot (C_{O_2,b} - C_{O_2,d}) + \frac{d\bar{\xi}_{Reg}}{dt} \cdot \frac{1}{M_{O_2}} \cdot (1 - \varepsilon_b) \cdot c_v \cdot \rho_p}{u_{mf} \cdot (1 - \varepsilon_b)} \quad (22)$$

where $\bar{\xi}_{Reg}$ is the average oxygen loading of the catalyst in the regenerator in g O₂/kg cat. The following expression is used to determine the change in the average oxygen loading of the catalyst in the regenerator per time unit:

$$\frac{d\bar{\xi}_{Reg}}{dt} = k_{ox} \cdot \bar{\xi}_{Reg}^{-3.8} \cdot \sqrt{p_{O_2}} \quad (23)$$

where k_{ox} is given by:

$$k_{ox} = 1,4 \cdot 10^{-3} \frac{g}{kg \cdot Pa^{0,5} \cdot s^{0,5}} \quad (24)$$

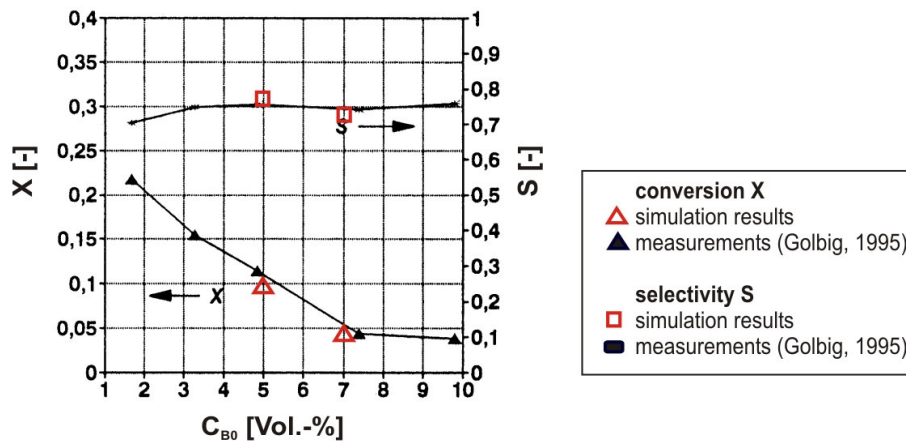


Fig. 9 Comparison of simulation results with measurements by Golbig [2]

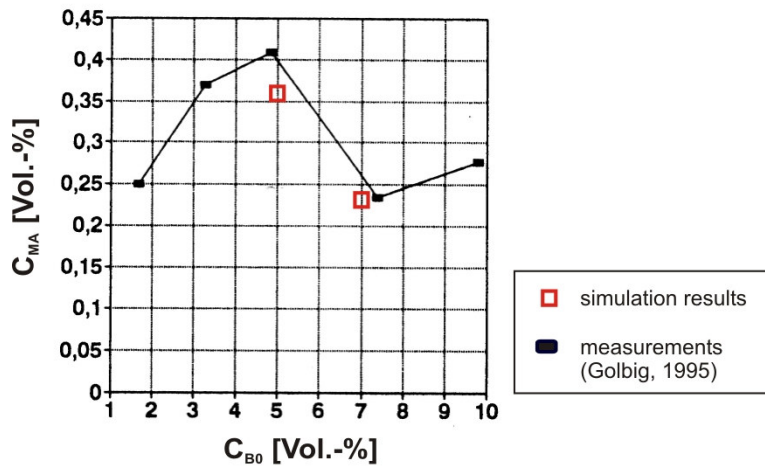


Fig. 10 Comparison of simulation results with measurements by Golbig [2]

Results

The reaction results are characterized by the n-butane conversion X and the selectivity S to the desired product MA. They are calculated from concentrations:

$$X = 1 - \frac{C_{B,H}}{C_{B,0}} \quad (25)$$

$$S = \frac{C_{MSA}}{C_{B,0} - C_{B,H}} \quad (26)$$

Fig. 9 compares the simulation results for the n-butane conversion and the selectivity S to the measurements by Golbig [5]. The n-butane concentration in the riser reactor feed is varied. The regenerator feed has 50mol% oxygen. There is a good agreement between the SolidSim simulation results and the Golbig measurements. Fig. 10 shows the volumetric MA concentration in the product gas for the same simulation runs and the measurements of

Golbig [5] for different n-butane concentrations. Again, there is a good agreement between the results of the SolidSim simulation and the Golbig measurements.

Variant: Enlarged regenerator volume

To test the influence of the regenerator volume on n-butane conversion the riser/regenerator configuration is changed: The regenerator diameter is increased by factor 2, the height of the bubbling bed is increased by factor 2.5 so that the 10fold regenerator bed volume is obtained. The simulation uses a 5mol% n-butane feed to the riser and a 50mol% oxygen feed to the regenerator. The simulation using the flowsheet simulation tool SolidSim yields a n-butane conversion of 48% as compared to 9.5% found in fig.9. The selectivity is also increased by 7 percent points to 84%.

This effect is due to a higher oxygen loading of the catalyst when it leaves the enlarged regenerator as the average residence-time of the catalyst in the regenerator is 10fold increased. However, the catalyst's oxygen-loading capacities must be sufficient to allow for higher oxygen loadings.

Due to the enlargement of the regenerator cross-sectional area a proportionally increased gas throughput is required. In addition a higher (about 9.5fold increased) catalyst mass is required in the system. As the catalyst is due to a complicated production process very expensive the latter point has a crucial effect on the costs for the proposed variant.

Discussion

The riser/regenerator system has been successfully modeled and calculated using the flowsheet simulation tool SolidSim. It has been shown that regenerator volume has a decisive effect on the n-butane conversion. Oxygen-load of catalyst is the limiting factor.

The model could be further refined by including the distributions of the chemisorbed oxygen over the catalyst particles. The residence time of particles differ depending on their particle size a lot due to the classifying effect of the entrainment. In this work simply the average mean oxygen loading has been used. Also, a more detailed reactor model could be used. However, the goal was not to build a most detailed model for the process under consideration but to demonstrate that realistic results can be obtained from using the process unit models of the general flowsheet simulation tool SolidSim.

Nomenclature

a	=	specific interfacial area, m^2/m^3
c_b, c_j	=	attrition rate constants, def. by equ. (12), (11)
c_v	=	solids volume concentration, -
C_b, C_d	=	reactant concentrations in bubble and dense phase, mol/m^3
d_{or}	=	orifice diameter, m
d_p	=	particle diameter, m
d_v	=	bubble volume equivalent sphere diameter, m
D	=	diffusion coefficient, m^2/s
h	=	height above gas distributor, m
k_G	=	mass transfer coefficient, m/s
k_m	=	reaction rate constant, $m^3/(kg s)$

m	=	mass, kg
\dot{m}	=	mass flow, kg/s
M	=	molar mass kg/m ³
n	=	number of particles, -
\dot{n}	=	particle flow, - /s
n_{or}	=	number of orifices in the gas distributor, -
N_p	=	number of particles, -
P	=	partial pressure, Pa
$Q_0(d_p)$	=	cumulative particle size distribution of number, -
$Q_3(d_p)$	=	cumulative particle size distribution of mass, -
$Q_2(d_p)$	=	cumulative particle size distribution of surface, -
S	=	selectivity, def. by equ.(26), -
t	=	time, s
u	=	superficial fluidizing velocity, m/s
u_b	=	local bubble rise velocity, m/s
u_{mf}	=	minimum fluidizing velocity (superficial), m/s
X	=	conversion rate, def. by equ.(25), -

Greek letters

ϵ_b	=	local bubble volume fraction, -
ϵ_{mf}	=	bed voidage at minimum fluidization conditions, -
ρ_p	=	appent density of bed particles, kg/m ³
ρ_f	=	gas density, kg/m ³
ξ	=	oxygen load of catalyst, g O ₂ / kg catalyst

Indices

att	=	Attrition
b	=	bed
B	=	Butane
E	=	Elutriation
F	=	Feed
H _b	=	height of bottom bed surface above distributor, m
i	=	number of particle size interval
MA	=	Maleic Anhydride

O	=	Overflow
O ₂	=	Oxygen
ox	=	catalyst oxidation
t	=	time
p	=	particle
R	=	Riser
Reg	=	Regenerator

References

1. Werther J, Wein J. Expansion behavior of gas fluidized beds in the turbulent regime. *AIChE Symposium Series*. 1994; 301:31-44.
2. Golbig KG, Werther J. Selective synthesis of maleic anhydride by spatial separation of *n*-butane oxidation and catalyst reoxidation. *Chem. Eng. Sc.* 1997;52:583-595.
3. Seider WD, Seader JD, Lewin DR. Process design principles: synthesis, analysis and evaluation, Hoboken, NY: John Wiley & Sons; 1999.
4. Hartge EU, Pogodda M, Reimers C, Schwier D, Gruhn G, Werther J. SolidSim – a tool for the flowsheet simulation of solids processes. *Aufbereitungstechnik* 2006; 47: 42-51
5. Golbig KG, Selektive Oxidation von n-Butan zu Maleinsäureanhydrid in der Zirkulierenden Wirbelschicht. Ph.D. thesis, Hamburg University of Technology. Düsseldorf: VDI Verlag; 1995
6. Hilligardt K, Werther J. The influence of Temperature and Solids Properties on the Size and Growth of Bubbles in Gas Fluidized Beds. *Chem. Eng. Technol.* 1987; 10: 272.
7. Davidson JF, Harrison D. *Fluidised Particles*; Cambridge University Press: Cambridge, U.K., 1963
8. Tasirin SM, Geldart D. Entrainment of FCC from Fluidized Beds – A New Correlation for the Entrainment Rate Constants. *Powder Technol.* 1998; 95:240.
9. Kunii D, Levenspiel O. Fluidization Engineering. Stoneham, MA: Butterworth-Heinemann; 1991
10. Werther J, Xi W, Jet attrition of catalyst in gas fluidized beds. *Powder Tech.* 1993; 76: 39
11. Xi W, Katalysatorabrieb in Wirbelschichtreaktoren, PhD dissertation, Technical University Hamburg-Harburg, Hamburg 1993.
12. Sit SP, Grace JR. Effect of Bubble Interaction on Interphase Mass Transfer in Gas Fluidized Beds. *Chem. Eng. Sci.* 1981; 36:327.

13. Sitzmann W, Werther J, Böck W, Emig G. Modelling of Fluidized Bed Reactors – Determination of Suitable Kinetics for Complex Reactions. *Ger. Chem. Eng.* 1985; 8:301.
14. Contractor R, Sleight AW. Maleic Anhydride from C4 Feedstocks using Fluidized Bed reactors. *Catalysis Today*, 1987;1:587-607
15. Contractor R, Butane Oxidation to Maleic Anhydride in a Recirculating SolidRiser Reactor. In: Basu P and Large JF, ed. *Circulating Fluidized Bed Technology II*. Proceedings of the 2nd International Conference on Circulating Fluidized Beds. Compiegne: Pergamon Press; 1988: 467-474
16. VDI-Heat Atlas, Düsseldorf: VDI Verlag; 1997

